Available online at www.sciencedirect.com
ScienceDirect
Catalysis Today 117 (2006) 498–505
CATALYSIS TODAY
www.elsevier.com/locate/cattod

Effect of the *Re* number on heat and mass transport in a catalytic monolith

Francesco Donsì [a,*], Almerinda Di Benedetto [b], Francesco S. Marra [b], Gennaro Russo [a]

[a] *Dipartimento di Ingegneria Chimica, Università degli Studi di Napoli "Federico II", P.le Tecchio 80, 80125 Napoli, Italy*
[b] *Istituto di Ricerche sulla Combustione-C.N.R., via Diocleziano 328, 80124 Napoli, Italy*

Available online 18 July 2006

Abstract

The numerical investigation of inter-phase heat transfer in a catalytic combustor, under laminar flow regime at different values of the *Re* number, is performed by means of a 2D axi-symmetric model of a single monolith channel. Numerical results highlight that axial diffusion comes to play an important role in the ignition region also at high convective fluxes (high *Re*) due to the strong flow perturbation accompanying light-off, with the consequences that: (a) the ignition position is not a linear function of contact time, as it would be expected at high *Re*; (b) the heat and mass transfer between surface and bulk gas phase are non-linearly affected by *Re*, especially in the entrance and in the ignition regions.

A previously developed correlation for *Nu* and *Sh* is, hence, extended to include the effect of the *Re* number on heat and mass fluxes, enabling the prediction of the local value of *Nu* and *Sh* in the main features, and in particular the enhancement in the ignition region and the dependence on *Re*.

Keywords: CFD; Catalytic combustor; Axial diffusion; Heat transfer; *Nu* correlation

1. Introduction

In a catalytic monolith, the occurrence of a fast superficial exothermic reaction strongly affects the inter-phase heat and mass transport. In the ignition region, it was found that the local values of the heat and mass transfer coefficients (*Nu* and *Sh*) exhibit a local enhancement [1–11].

Gupta and Balakotaiah addressed such local increase to numerical inaccuracies [1]; nevertheless, we recently showed that it has a strong physical meaning and is generated analogously to the entrance effects by the renewed development of local radial gradients of temperature, concentration and velocity [4,10,11]. The fast rate of heat production associated to the light-off of a surface exothermic reaction is indeed capable of producing a perturbation, whose effects are comparable to entrance effects [4,10,11], and that, hence, has to be taken into account when predicting the wall fluxes (*Nu* and *Sh*) in 1D modeling of monolithic reactors.

Until now, the transfer coefficients have been calculated as the interpolation of two curves (Nu_H and Nu_T), to which the local transfer coefficient tends far from the ignition region: prior to ignition, reactive *Nu* (*Sh*) tends to the constant wall heat flux curve (Nu_H), while downstream of the ignition region it tends to the constant wall temperature curve (Nu_T) [1–9].

We showed that in the presence of a surface reaction, the catalytic channel could be conceptually divided into two zones, which are both characterized by the development of momentum, heat and mass boundary layers. In the first zone, the radial gradients are perturbed by the entrance effects, while in the second zone, the radial gradients are influenced by ignition [11]. Extension and position of these two zones may vary, sometimes overlapping, in dependence on the parameters [4,10,11].

In the literature, the effect of fluid flow on *Nu* number in laminar regime in absence of reaction was taken into account by plotting *Nu* versus the dimensionless axial coordinate $x^* = x/(2 \times R \times Re \times Pr)$ [12], reckoning that Nu_H or Nu_T evaluated at different *Re* overlap for values of the Peclet number ($Pe = Re \times Pr$) larger than the conventional limit of 50 [12], while for $Pe < 50$, a certain displacement is observed [13].

Recently, by means of CFD analysis, we demonstrated that when coupling with the fluid flow is properly taken into account, the axial diffusion of momentum and heat may be

* Corresponding author. Tel.: +39 081 7682947; fax: +39 081 7629415.
E-mail address: fradonsi@unina.it (F. Donsì).

0920-5861/$ – see front matter © 2006 Elsevier B.V. All rights reserved.
doi:10.1016/j.cattod.2006.06.005

Nomenclature

c_P	specific heat (kJ/kg K)
C_{tot}	total concentraton (mol/m^3)
D	diffusion coefficient (m^2/s)
Da_t	Transverse Damköhler number
H, H_i°, h_s	enthalpy (J/kg)
$J_{r,i}$, $J_{x,i}$	radial and axial mass flux of species i (m/s)
k°	kinetic constant (mol/m^2 s)
Le	Lewis number
L	channel length (m)
N_s	species number
Nu	Nusselt number
p	pressure (Pa)
Pr	Prandtl number
r	radial coordiante (m)
R	channel radius (m) or universal gas constant
Re	Reynolds number
Sc	Schmidt number
Sh	Sherwood number
t	time coordinate (s)
T	temperature (K)
u	longitudinal component of velocity (m/s)
v	radial component of velocity (m/s)
x^*	dimensionless axial coordinate, $x/(2 \times R \times Re \times Pr)$
x	axial coordinate (m)
y	mass fraction

Greek letters

ΔE	activation energy (J/mol)
μ	viscosity (Pa s)
ρ	density (kg/m^3)
τ	stress tensor (kg/m s^2)
ω	reaction rate (mol/m^2 s), heat of reaction (J/mol s)

Subscripts and superscripts

ad	adiabatic
b	bulk
c	convective
C_3H_8	propane
h	heat
H	constant heat flux
in	inlet
lo	light-off location
r	radial direction
T	constant temperature
w	wall
y	mass
x	axial direction

relevant with respect to axial convection, also at $Pe > 50$. This result was addressed to the modification of the characteristic times of axial convection and diffusion following the arising of a strong radial component of velocity [14], which affects the gas residence time in the proximity of the wall.

The aim of the present paper is to give insights on the role of the axial diffusion both on the inter-phase heat transfer efficiency and on the ignition location in a monolithic catalytic combustor, at varying the Pe number, through the variation of Re, at a fixed value of Pr number ($Pr = 0.7$), by taking into account the full coupling between energy, mass and momentum balance equations.

2. Model

A two-dimensional axi-symmetric model, previously developed [4,10,11], has been adopted to simulate the behavior of a single circular channel (length $L = 0.12$ m; radius $R = 0.00045$ m) of an adiabatic monolith reactor, in which a superficial reaction occurs. The mass and energy balance equations are solved, coupled to the Navier–Stokes equations. The balance equations are written in cylindrical coordinates and they read:

Continuity equation:

$$\frac{\partial \rho}{\partial t} + \frac{\partial \rho u}{\partial x} + \frac{1}{r}\frac{\partial r \rho v}{\partial r} = 0 \tag{1}$$

Momentum balance equation in the axial coordinate:

$$\frac{\partial \rho u}{\partial t} + \frac{\partial \rho u u}{\partial x} + \frac{1}{r}\frac{\partial r \rho v u}{\partial r} = -\frac{\partial p}{\partial x} + \frac{1}{r}\frac{\partial r \tau_{xr}}{\partial r} + \frac{\partial \tau_{xx}}{\partial x} \tag{2}$$

Momentum balance equation in the radial coordinate:

$$\frac{\partial \rho v}{\partial t} + \frac{\partial \rho u v}{\partial x} + \frac{1}{r}\frac{\partial r \rho v v}{\partial r} = -\frac{\partial p}{\partial r} + \frac{\partial \tau_{xr}}{\partial x} + \frac{1}{r}\frac{\partial r \tau_{rr}}{\partial r} \tag{3}$$

Specie mass balance equation:

$$\frac{\partial \rho y_i}{\partial t} + \frac{\partial \rho u y_i}{\partial x} + \frac{1}{r}\frac{\partial r \rho v y_i}{\partial r} = \frac{\partial}{\partial x}(J_{x,i}) + \frac{1}{r}\frac{\partial}{\partial r}(r J_{r,i}), \quad i = 1, \ldots, N_s - 1 \tag{4}$$

Energy balance equation:

$$\frac{\partial \rho h}{\partial t} + \frac{\partial \rho u h}{\partial x} + \frac{1}{r}\frac{\partial r \rho v h}{\partial r} = \frac{\partial}{\partial x}\left(k(T)\frac{\partial T}{\partial x}\right) + \frac{1}{r}\frac{\partial}{\partial r}\left(r k(T)\frac{\partial T}{\partial r}\right) + \frac{\partial p}{\partial t} \tag{5}$$

where $h = c_p(T)T + \sum_{i=1}^{N_S} y_i H_i^0 + p/\rho + (u^2 + v^2)/2$, and N_s is the number of species that form the gas mixture. Diffusive mass fluxes $J_{x,i}$ and $J_{r,i}$ are computed as:

$$J_{z,i} = \mu\, Sc\, \frac{\partial y_i}{\partial x}, \quad z = r, x \tag{6}$$

where $Sc = 0.7$ is a fixed Schmidt number and μ is the dynamic viscosity. Ideal gas law completes the model.

The boundary conditions are listed in the following.

At the inlet we assumed the *Dirichlet* type boundary conditions:

$$@ \quad x = 0 \text{ and } 0 < r < R: \quad u = u_{in}, \quad v = 0, \quad T = T_{in}, \quad y_i = y_{i,in} \tag{7}$$

$$@ \quad x = L \text{ and } 0 < r < R_1: \quad \frac{\partial u}{\partial r} = v = \frac{\partial T}{\partial r} = \frac{\partial y_i}{\partial r} = 0; \tag{8}$$

$$@ \quad 0 < x < L \text{ and } r = 0: \quad \frac{\partial u}{\partial r} = v = \frac{\partial T}{\partial r} = \frac{\partial y_i}{\partial r} = 0; \tag{9}$$

$$@ \quad 0 < x < L \text{ and } r = R: \quad u = v = 0$$

At the wall (@ $0 < x < L$ and $r = R$) the reaction rate occurs:

$$u = v = 0, \quad k\frac{\partial T}{\partial r}\bigg|_{R-} = \frac{\sum_i h_i J_i}{\rho_{\text{wall}} D_{\text{wall}}}, \quad \frac{\partial T}{\partial r}\bigg|_{R+} = 0, \qquad J_{r,i}|_{R-} = \omega_{y,i} \tag{10}$$

The source term $\omega_{y,i}$ is the reaction rate of species i. The model reaction is the catalytic combustion of propane. The reaction rate is assumed to be a one step irreversible reaction zeroth order with respect to oxygen and first order with respect to propane mass fraction as following:

$$\omega_{y,C_3H_8} = k_0 \exp\left(-\frac{\Delta E}{\bar{R}T}\right) y_{C_3H_8} \tag{11}$$

The values of the adopted kinetic parameters are $k_0 = 10^6$ mol/m^2 s, $\Delta E/\bar{R} = 10,900$ K [10,11].

All properties and transport coefficients are computed by means of multi-component mixture approaches. Specific heats of the species are determined from the Janaf tables.

From the computed solution of the numerical model, radial average gas temperature was calculated according to the following formula:

$$T_b = \frac{\int_0^R \rho c_p T u r \, dr}{\int_0^R \rho u c_p r \, dr} \tag{12}$$

Nu number was calculated at bulk conditions, according to the following formula:

$$Nu = \frac{k(T_w)}{k(T_b)} \frac{2R}{T_w - T_b} \frac{\partial T}{\partial r}\bigg|_{r=R} \tag{13}$$

where T_w is the gas temperature computed at the wall.

Numerical solutions of the equations have been performed by means of the commercial software package CFD-ACE+ [15]. The resulting system of non-linear algebraic equations has been solved following the SIMPLEC method [16]. The grid was chosen to be finer in the zone of light-off along the axial direction, and in the proximity of the wall along the radial direction. The grid was adapted to the changes of the *Re* number that determine a variation of the light-off point location.

3. Results

Numerical simulations were carried out at constant $Pr = 0.7$, varying *Re* between 160 and 1000 and hence $Pe = Re \times Pr$ between 113 and 700.

3.1. Ignition

Light-off position is identified by the transition from the kinetic to the mass transfer controlled regime and by the steep increase of the wall temperature up to the adiabatic temperature. Both these criteria are presented in Fig. 1, in the form of the transverse Damköhler number Da_t (the ratio between the diffusive time and the kinetic time, as reported in Eq. (14)) and the wall temperature T_w, plotted versus the dimensionless axial coordinate x^*, for different values of *Re* number.

$$Da_t = \frac{k_0 \exp(-(\Delta E/\bar{R}T))R}{C_{tot} D_{C_3H_8}} \tag{14}$$

Small values of Da_t (kinetic time $\gg$ convective time) indicate that the reaction rate is controlled by the intrinsic kinetics of the surface reaction. This condition occurs for any *Re* number prior to light-off. Downstream of the ignition location, in consequence of the steep increase of the surface temperature, the rate of the catalytic reaction is greatly

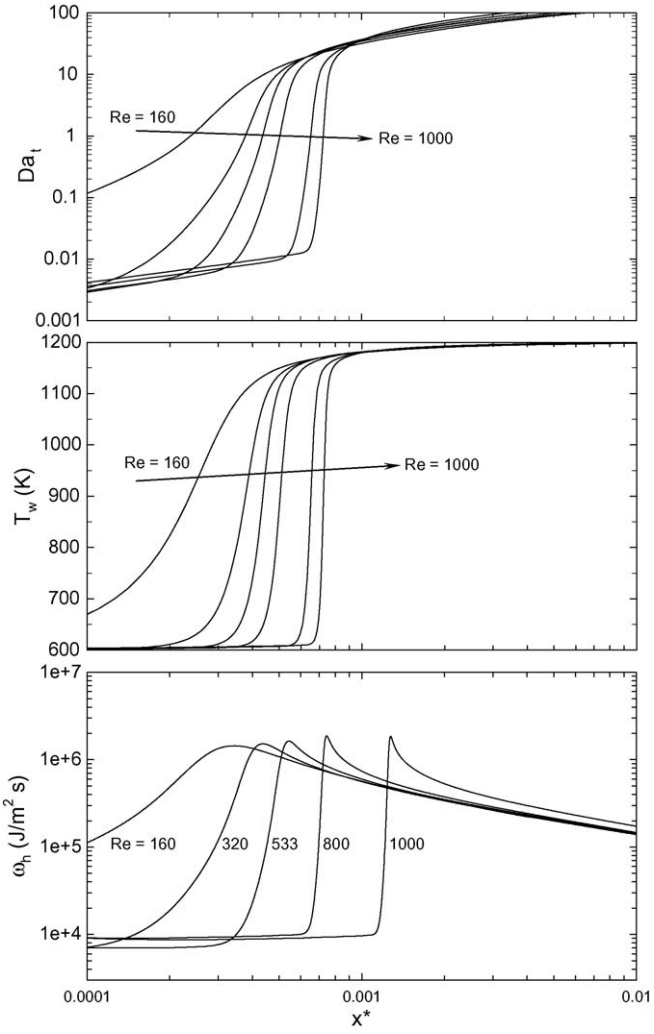

Fig. 1. Transverse Damköhler number Da_t, wall temperature T_w and heat flux at the wall ω_h, as function of the dimensionless axial coordinate x^* at varying *Re* between 160 and 1000.

enhanced (as shown in Fig. 1, in terms of ω_h, rate of heat production at the wall), Da_t jumps up to very large values (kinetic time $\ll$ diffusive time) and inter-phase mass and heat transfer becomes the rate determining mechanism (Fig. 1).

Noticeably, the location of the ignition exhibits a significant displacement along $x^* = x/(2 \times R \times Re \times Pr)$ at varying Re, shifting to higher x^* at increasing Re (Fig. 1). This implies that the actual axial location of the ignition in dimensional form (x_{lo}) is not a linear function of Re, but increases more rapidly than Re.

This concept is clarified in Fig. 2, where the light-off axial position x_{lo} (conventionally calculated as the point at which the axial wall temperature derivative reaches its maximum) is plotted versus the Re number. Numerical results show that x_{lo} effectively does not depend linearly on Re, but exhibits a quadratic dependence. This is quite surprising because at large Re a different behavior would have been expected. When axial diffusion can be neglected in comparison with axial convection (this condition is conventionally indicated in $Pe > 50$, which for $Pr = 0.7$ corresponds to $Re > 71$) the contact time is proportional to Re, and also the heat transfer efficiency is also proportional to Re (Nu curves collapse on a single curve when plotted versus x^* at large Re) [12]. Since, the kinetic time is maintained constant (constant kinetics of the surface reaction), the light-off position should be a linear function of the contact time, and hence, of Re [17]. Nevertheless, numerical results, reported in Fig. 2, show that x_{lo} is a quadratic function of Re. We have addressed this behavior to the relevance of heat axial back diffusion, as it is discussed below.

We have recently proved that the axial diffusion may come to play a significant role even at high Re, when strong components of radial velocity arises, perturbing the flow field and the residence time distribution close to the wall, similarly to what happens in the entrance region. In the inlet region of a circular channel ($x^* < 10^{-3}$), where entrance effects are especially vigorous at lower Re, the axial diffusion is significant for Re as high as 1600, resulting in a strong influence on the heat transfer efficiency [14].

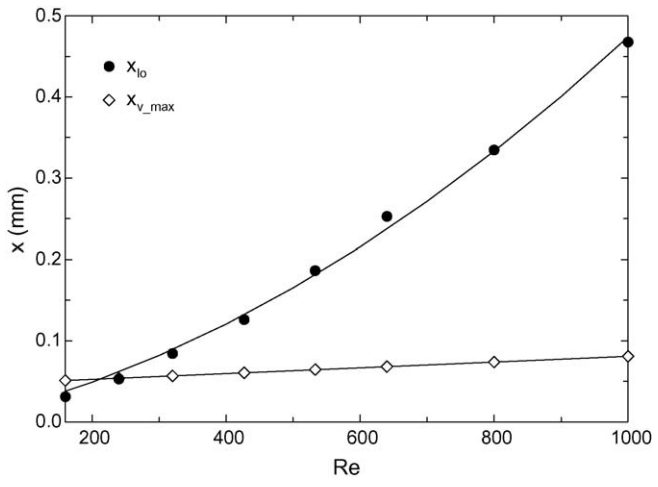

Fig. 2. Position of light-off and of the highest radial velocity (v_{max}) due to the entrance effects as function of Re number.

To get an idea of the extension of the reactor where the entrance effects play the major role, in Fig. 2 the locus of the peaks of the radial velocity component (x_{v_max}) due to the entrance effects and obtained for the non-reactive case, are also reported: the flow perturbation deriving from the development of the velocity profile can be considered to extend on a double distance with respect to the peak location.

Hence, with the help of Fig. 2, two regimes may be identified at varying Re. The first regime occurs when the ignition lays within the region of strong flow perturbation due to entrance effects ($Re < 400$). The second regime occurs when ignition lays downstream of the main entrance effects ($Re \geq 400$): a quadratic law still rules the dependence of the light-off position on Re, suggesting that also under this condition the axial gas diffusion plays a relevant role.

Indeed, downstream of the entrance region, the ignition region is subject to developing flow conditions and is still affected by strong radial gradients of momentum, heat and mass. Fig. 3 reports the radial velocity components in the channel at different Re numbers. When ignition occurs within the entrance region ($Re < 400$), the flow perturbations due to the entrance effects and to the reaction ignition overlap, leading to a single peak of v, as shown for $Re = 160$, where the ignition occurs at $x^* = 3.5 \times 10^{-4}$ (Fig. 3). When the ignition takes place downstream of the entrance region ($Re \geq 400$), the two flow perturbations do not overlap, and two peaks of v can be distinguished. This condition is exemplified in Fig. 3 by the plots at $Re = 533$, where the ignition occurs at $x^* = 5.5 \times 10^{-4}$ and $Re = 1000$, where the ignition occurs at $x^* = 7.4 \times 10^{-4}$.

According to the results of Figs. 2 and 3, at lower Re, the two zones overlap, while at higher Re they are clearly separate. In any case, both at low and at high Re numbers, the ignition is always accompanied by a developing fluid flow and in particular by the arising of a radial component of velocity (v). The presence of v is the cause for the residence time of the fluid element travelling close to the wall to increase: a sort of bubble is created in correspondence of the ignition point generated by the heat production. In agreement with our previous findings, the deviation of the streamlines and the increase of the residence time in the proximity of the wall increase the relevance of the axial diffusion of momentum heat and mass even at high Re numbers. In particular, axial back diffusion of heat increases the heat transfer efficiency especially at lower Re, shifting upstream the ignition location [14].

In the ignition region, the wall temperature and the consumption of reactants increase very rapidly, determining the formation of strong heat and mass gradients in both the axial and the radial direction. In concurrence, the increase in bulk temperature and conversion takes place with a smooth slope.

Noticeably, the bulk gas is heated with higher efficiency at lower Re. This can be better appreciated in Fig. 4, where the highest temperature difference between wall and bulk phase ($\Delta T_{max} = T_w - T_b$), corresponding to the temperature difference at the light-off, is plotted as a function of Re. ΔT_{max} attains

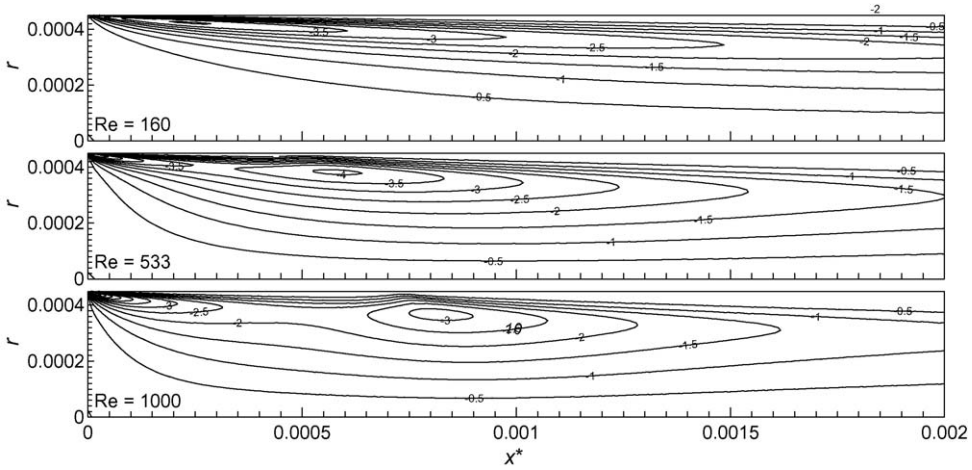

Fig. 3. Contour plots of the radial velocity (v) profiles along x^* at Re = 160, 533 and 1000.

large values (around 500 K) and exhibits an increasing trend at increasing *Re*, suggesting that gas pre-heating is more efficient at lower *Re* numbers. The more efficient pre-heating of the gas is the combination of the larger relevance of axial back diffusion of heat and of the radial heat transfer between the surface and the bulk.

3.2. Heat transfer efficiency

The heat transfer efficiency between the wall and the bulk gas phase, measured by the computed *Nu* numbers (Eq. (13)), has been reported in Fig. 5, versus the dimensionless coordinate x^* for different values of *Re*. Since Lewis number ($Le = Sc/Pr$) is always equal to unity in the present work, *Sh* is roughly analogous to *Nu* and hence is not discussed in details. *Nu* curves do not overlap when plotted versus x^*, even at high *Re* numbers, exhibiting in the light-off region a strong enhancement in heat transfer efficiency, as previously reported by other authors [2–11]. Fig. 5 also shows that in correspondence of the ignition, the heat transfer efficiency is higher at higher *Re*, but in the region just upstream of the ignition location *Nu* is higher at lower *Re* due to the larger contribution of axial back diffusion, thus, allowing a more efficient pre-heating of the gas.

In Fig. 5, *Nu* is also compared with the Nu_H and Nu_T curves, as calculated from heat exchangers simulations, with

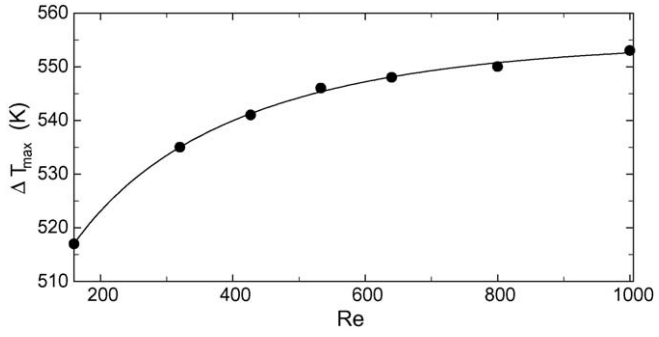

Fig. 4. Temperature difference at the ignition (ΔT_{max}) as a function of *Re*.

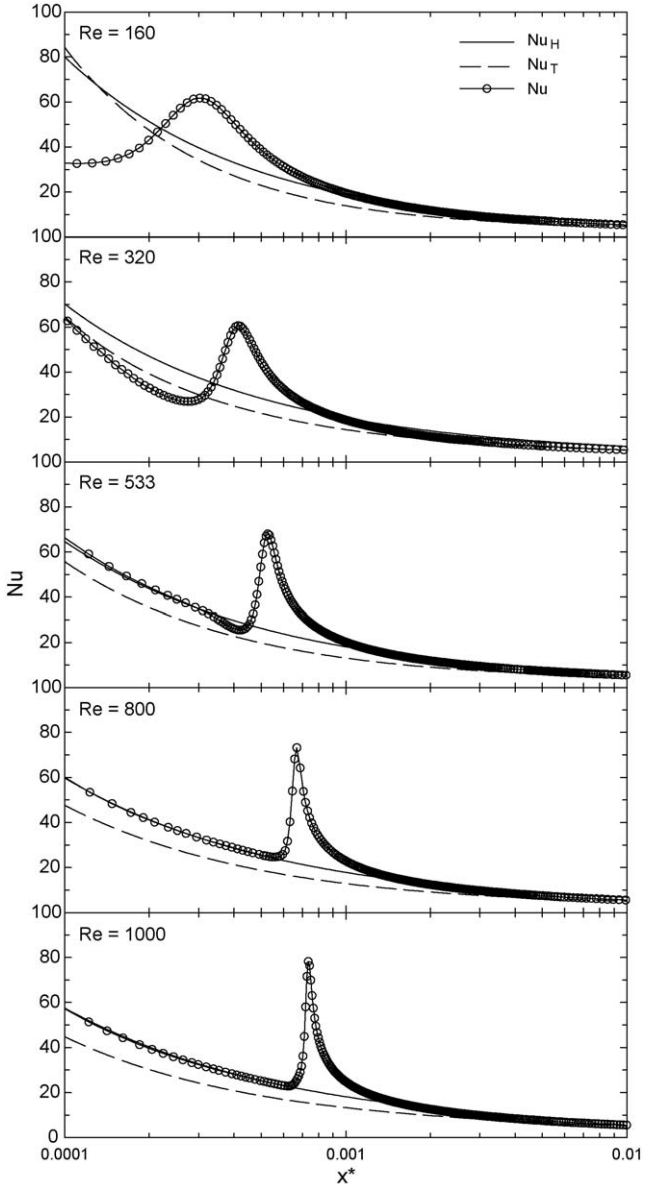

Fig. 5. *Nu* in the presence of reaction, Nu_T and Nu_H and the axial heat flux as function of x^* at different values of *Re*.

the same inlet boundary conditions (Dirichlet type) [14]. The effect of axial diffusion of heat and momentum and their role played at different *Re* are both evident: the lower *Re*, the stronger the enhancement of transfer efficiency (*Nu*) that shifts backwards the light-off location. In consequence, Nu_T and Nu_H curves, which also depend on *Re*, represent the asymptotes of the *Nu* curve for the reactive case only at high *Re* number ($Re \geq 533$). At low *Re* values ($Re < 533$), *Nu* does not overlap Nu_H in the inlet section before ignition. Indeed, the rate of heat production at the wall (ω_h), reported in Fig. 1, at varying *Re*, does not attain a constant value with the consequence that the analogy with the constant wall heat flux exchanger fails.

The wall heat flux at low values of *Re* increases along the channel as the heat back diffusion raises the temperature upstream of the ignition, thus, increasing also the reaction rate. This is particularly evident for *Re* = 160 and 320, where prior to ignition both the wall temperature and the wall heat flux increase: *Nu* reflects the transitional state of the wall boundary conditions (Fig. 1).

From these results, it appears that at low values of the *Re* numbers, in addition to the constant flux zone and the constant temperature zone defined in our previous paper [11], a third zone can be identified, which represents the transition from the constant flux to the constant wall temperature case. The width of this zone is negligible at very high *Re* numbers (*Re* = 1000, Figs. 1 and 5) and becomes wider on decreasing the *Re* number. At low values of *Re*, the first zone disappears and a transition zone arises in which neither the constant heat flux at the wall nor the constant wall temperature conditions hold. On increasing the *Re* number, the first zone emerges, since the wall heat flux can be considered with good approximation constant before ignition, while the transition zone becomes narrower.

Downstream of the ignition point for any *Re*, the heat transfer efficiency resembles that attained in the entry region of a heat exchanger with constant wall temperature, as shown by the good agreement of the decreasing *Nu* branch far downstream of ignition and the Nu_T curve.

In our previous paper, we derived a correlation of *Nu* which takes into account also its local enhancement [4,11]. In the following, we extend the validity of the correlation also at varying *Re* number.

3.3. Correlation for Nu number in the presence of reaction

Groppi and co-workers expressed by means of the Fetting formula, a correlation for the determination of *Nu* number in the presence of reaction (Eq. (15)) [8,9]. *Nu* jumps from the Nu_H curve to the Nu_T curve in dependence of the value of the Damköhler number (Da_t in Eq. (14)) locally attained along the channel. Before ignition, where $Da_t \ll 1$, *Nu* coincides with Nu_H, while after the ignition ($Da_t \gg 1$) *Nu* coincides with Nu_T.

$$\frac{Nu - Nu_H}{Nu_T - Nu_H} = \frac{Da_t Nu}{(Da_t + Nu)Nu_T} \tag{15}$$

In the ignition region, the local *Nu* enhancement is not described by such correlation, which for a highly exothermic reaction in an adiabatic reactor may lead to significant errors [8]. We modified Eq. (15) to take into account the *Nu* enhancement occurring in the ignition region by replacing Nu_T with Nu_{ad} [4,10,11], where Nu_{ad} is defined over the difference between the adiabatic temperature and the bulk temperature (Eq. (16)).

$$Nu_{ad} = \frac{-(\partial T/\partial r)|_{r=R} 2R}{(T_{ad} - T_b)} \frac{k_w}{k_b} \tag{16}$$

The modified correlation is represented by Eq. (17).

$$\frac{Nu - Nu_H}{Nu_{ad} - Nu_H} = \frac{Da_t Nu}{(Da_t + Nu)Nu_{ad}} \tag{17}$$

Nu_{ad} may be calculated as a function of the dimensionless temperature gradient $\Delta T_b = (T_{ad} - T_b)/\Delta T_{ad}$, and collapse at varying the operating conditions when plotted as function of ΔT_b [4].

Nevertheless, Nu_{ad} curves at different values of the *Re* numbers do not overlap (Fig. 6). On increasing the *Re* number, Nu_{ad}, and hence, the heat transfer efficiency, is higher as the back-diffusion effects are lower and the gradients of temperature and velocity are steeper. This result is in agreement with our previous findings on the heat exchangers problem with slip wall boundary conditions [14]. In order to drive the Nu_{ad} curves to a good overlapping, the dimensionless temperature gradient was modified ($\Delta T'_b$) as reported in Eq. (18), to take into account the effects of the kinetics and inlet conditions, by means of dimensionless adiabatic temperature rise *B* (Eq. (19)), of the dimensionless activation energy γ (Eq. (20)) of Da_t (Eq. (14)) and of *Re*, by means of *Pe*.

$$\Delta T'_b = B^a \gamma^b Da_t^{in^c} (Pr \times Re)^d \Delta T_b \tag{18}$$

$$B = \frac{\Delta T_{ad}}{T_{in}} \tag{19}$$

$$\gamma = \frac{\Delta E}{\bar{R} T_{in}} \tag{20}$$

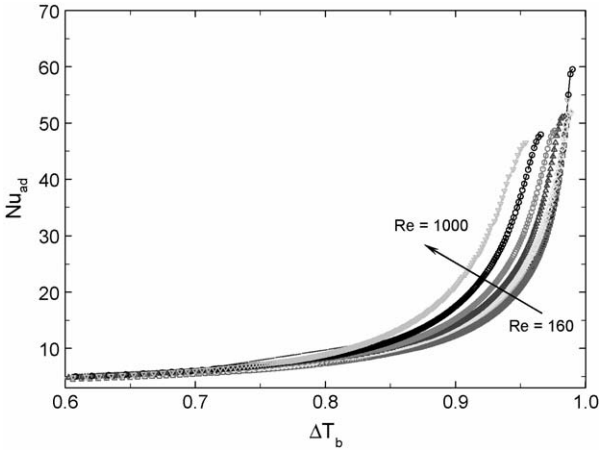

Fig. 6. Nu_{ad} as function of ΔT_b at different values of *Re*.

By correlating all the simulations data, we found that the best correlation is achieved with the following values of the constants embedded in $\Delta T'_b$: $a = 0.08$, $b = 0.015$, $c = 0.02$, $d = 0.03$. The Nu_{ad} curves collapse when plotted versus $\Delta T'_b$ at varying the *Re* number (160–1000), the inlet propane concentration (0.015–0.03), the inlet temperature (575–650 K), the pre-exponential factor ($k_0 = 5 \times 10^5$–5×10^6 mol/m^2 s) and the activation energy ($\Delta E/\bar{R} = 9800-11,300\,\mathrm{K}^{-1}$). The dependence of Nu_{ad} on $\Delta T'_b$ is expressed by Eq. (21).

$$Nu_{ad} = 3.656 + 1.95 \times 10^{-4} e^{11.2\,\Delta T'_b/(0.9-1.03\,\Delta T'_b)} \quad (21)$$

In Fig. 7, the computed *Nu* number is plotted versus x^* at different values of the *Re* number in comparison with the *Nu* numbers derived from the correlation, herein proposed (Correlation 1, Eqs. (17)–(21)) and the Fetting formula (Correlation 2, Eq. (15)). Remarkably, both in Eqs. (15) and (17), Nu_H and Nu_T have to be calculated as function of the *Re* number, as we previously claimed [14].

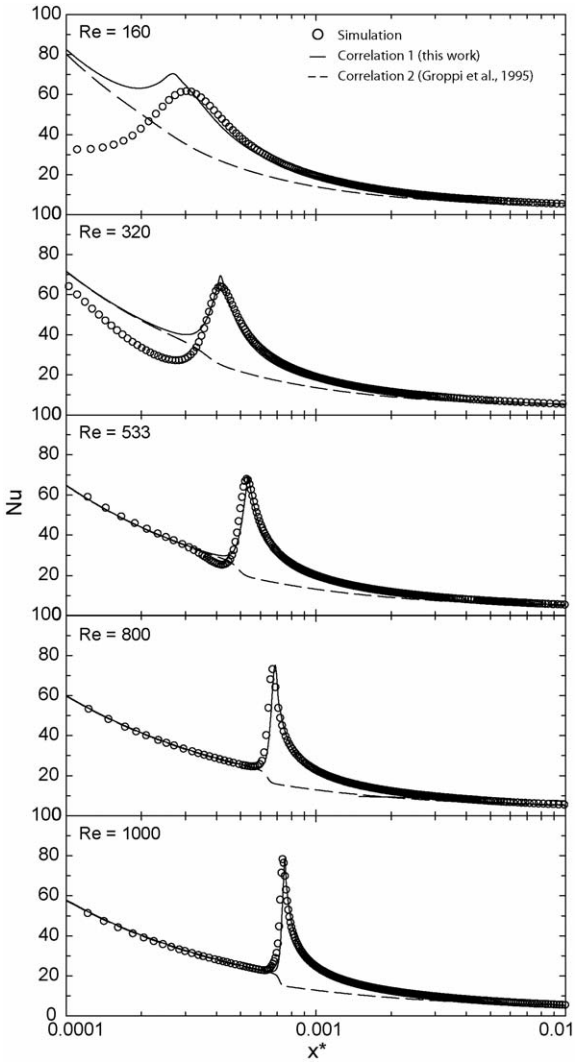

Fig. 7. *Nu* as a function of x^* at different values of *Re* as obtained by numerical simulations (symbols) and as predicted by the correlation proposed in this work (Correlation 1) and by the correlation reported in literature (Correlation 2 [8,9]).

When ignition occurs in the entrance region ($Re < 533$), both correlations do not reproduce the *Nu* trend in the entrance region, but Correlation 1 gives a significantly better approximation of the post-ignition branch, which is instead underpredicted by Correlation 2. At higher values of *Re*, when ignition occurs downstream of the entrance region, Correlation 2 is able to reproduce only the branches of *Nu* far from the ignition region (for $Da_t \ll 1$ and $Da_t \gg 1$), while Correlation 1 reproduces quite well also the local enhancement of the heat transfer efficiency in the ignition region (Fig. 7), which is of paramount importance also in the accuracy of the prediction of light-off location.

4. Conclusions

The numerical investigation of inter-phase heat transfer in a catalytic combustor under laminar flow regime at different values of the *Re* number, confirmed the relevance of the interdependence of the fluid dynamics, heat exchange and superficial reaction.

Especially in the region of ignition, the rapid gas expansion due to the exothermicity and fast rate of the catalytic reaction produces a strong perturbation of the gas phase which in turns gives rise to strong gradients of temperature, concentration and velocity. Hence, the axial diffusion of heat, mass and momentum becomes significant also at gas velocity higher than the conventional limit for neglecting axial diffusion ($Pe > 50$).

The role played by axial diffusion in the developing flow, accompanying ignition influences both the ignition location and the heat transfer efficiency. Numerical results show that the ignition location is not a linear function of *Re*, as it would be expected at very high *Re* values, but a quadratic function due to the more favorable gas pre-heating, also at high values of *Re*.

In addition, two regions may be identified on the basis of heat transfer efficiency, whose extension is determined by axial diffusion: in the first zone, due to the slow change of the reaction rate, constant heat flux conditions apply at the reactor wall and the Nu_H curve represents the *Nu* asymptote for the reactive case; in the second zone, downstream of ignition, where the wall temperature is constant and equal to the adiabatic temperature, the heat transfer tends to the Nu_T curve.

In the transition from the first zone to the second zone, corresponding to the ignition region, due to the rapid increase of the heat production rate and of the wall temperature, neither constant wall heat flux nor constant wall temperature conditions apply.

To take into account these findings, a correlation, previously proposed for *Nu*, has been extended to include the effect of the *Re* number. The extended correlation is capable of describing both the heat transfer enhancement in the ignition and the *Nu* dependence on the *Re* number.

Future work will be devoted to the comparison of the 1D model results in term of light-off position and wall temperature as obtained by means of the literature and the present correlation.

References

[1] N. Gupta, V. Balakotaiah, Chem. Eng. Sci. 56 (2001) 4771.
[2] L.C. Young, B.A. Finlayson, AIChE J. 22 (1976) 343.
[3] R.H. Heck, J. Wei, J.R. Katzer, AIChE J. 22 (1976) 477.
[4] A. Di Benedetto, F.S. Marra, G. Russo, Chem. Eng. Sci. 58 (2003) 1079–1086.
[5] A. Barresi, M. Vanni, G. Baldi, Proceeding of CHISA '96. Twelfth International Congress of Chemistry and Process Engineering, Praha, 1996.
[6] R.E. Hayes, S.T. Kolackowski, Catal. Today 47 (1999) 295.
[7] R.E. Hayes, S.T. Kolaczkowski, Chem. Eng. Sci. 49 (1994) 3587.
[8] G. Groppi, E. Tronconi, P. Forzatti, Catal. Rev.—Sci. Eng. 41 (1999) 227.
[9] G. Groppi, A. Belloli, E. Tronconi, P. Forzatti, Chem. Eng. Sci. 50 (1995) 2705.
[10] A. Di Benedetto, F. Donsì, F.S. Marra, G. Russo, Combust. Theor. Model. 9 (2005) 463.
[11] A. Di Benedetto, F. Donsì, F.S. Marra, G. Russo, AIChE J. 52 (2006) 911.
[12] R.K. Shah, A.L. London, Laminar Flow Forced Convection in Ducts, Academic Press, New York, 1978.
[13] G. Pagliarini, Int. J. Heat Mass Transfer 32 (1989) 1037.
[14] F. Donsì, A. Di Benedetto, F.S. Marra, G. Russo, Int. J. Chem. React. Eng. 3 (2005) A36.
[15] CFD-RC, CFD-ACE+ User Manual, http://www.esi-cfd.com, Huntsville, USA, 2004.
[16] J.P. Van Doormaal, G.D. Raithby, Numer. Heat Transfer 7 (1984) 147.
[17] K. Ramanathan, V. Balakotaiah, D.H. West, Chem. Eng. Sci. 58 (2003) 1381.